JOURNAL OF APPLIED ELECTROCHEMISTRY 20 (1990) 427–437

Electrochemical hydrodynamics in magnetic fields with laser interferometry: Influence of paramagnetic ions

R. N. O'BRIEN

Department of Chemistry, University of Victoria, Victoria, British Columbia, Canada V8W 2Y2

K. S. V. SANTHANAM

Chemical Physics Group, Tata Institute of Fundamental Research, Colaba, Bombay 400 005, India

Received 21 March 1989; revised 7 July 1989

The electrochemical reduction of Zn^{2+} was studied galvanostatically at current densities ranging from 0.10 to 7.0 mA cm^{-2} by using the system $Zn/ZnSO_4/Zn$, and operating it at its natural pH, under the influence of imposed non-variant magnetic field strengths ranging from 0.09 to 0.50 T in the V-position, C/A-position and A/C-position. The convective contours were visibly defined in the V- and A/C positions. The extent of convection in the C/A-position was negligible in the presence of the applied magnetic field. The presence of a paramagnetic ion (Mn^{2+} or Cr^{3+}) in the medium produced noticeable deviations in the concentration gradients. The mass transport coefficient for Zn^{2+} was evaluated in the presence of the applied magnetic field. The fluid flow velocities in the reduction of Zn^{2+} under the imposed magnetic field were estimated at 1–7 cm s^{-1}. The diffusion layer relaxation was followed by the fringe shift, after the electrolysis had terminated. The relaxation mechanism appears to be a slow rotational and translational movement of the paramagnetic fluid in the C/A-position. The exact mode of interaction between the magnetohydrodynamic effect, studied previously, and the paramagnetic effect studied in this work is not yet obvious. It is proposed that the mechanism by which energy dispersion is limited and momentum conserved is by suppression of microturbulence in the non-variant magnetic field.

1. Introduction

Previous papers [1, 2] reported the observation and analysis of the magnetic field effect on the electrochemical system $Cu/CuSO_4/Cu$ with plane parallel electrodes oriented in the vertical (V-), and other configurations. By the use of multiple-beam laser interferometry, a series of distorted fringes in the V-position were generated at the electrode–solution interface upon application of an external magnetic field; this distortion was greater at higher current densities, due to the increased velocity of the fluid flow which ranged from 1 to 13 cm s^{-1}. This distortion and the velocity of suspended particles also increased with increasing field. The convective effect was also observed when the anode was placed over the cathode (A/C configuration); in this configuration the magnetic field operated to reduce the apparent convection. With the electrodes arranged in these configurations, Cu dissolved by a 2e oxidation at the anode, $Cu \rightarrow Cu^{2+} + 2e^-$, and at the cathode Cu^{2+} was reduced via $Cu^{2+} + 2e^- \rightarrow Cu$. In the V-position the fluid flow was downwards at the anode and upwards at the cathode in a closed loop within the cell. Using the right-hand rule for generation of a force by a current flowing in a magnetic field, an increased flow upward and across the cathode should result, with the opposite force at the anode. In the A/C configuration the electrolyte at the top of the cell (anode region) is more dense and flows downward as the less dense cathode solution rises through it at intervals, forming regions of turbulance akin to Bénard cells. The hydrodynamic effect would be expected to be minimal when the cell electrodes are oriented in the C/A configuration. A reduced mass transport effect was, in fact, observed and was postulated as arising from the characteristics of a paramagnetic fluid; that is, a solution of the d^9 ion Cu^{2+}. With a view to obtaining further support for this postulate, we investigated the $Zn/ZnSO_4/Zn$ system (Zn^{2+} is d^{10}) by introducing paramagnetic ions into the medium. Mn^{2+} (d^5) and Cr^{3+} (d^2) were selected as they can satisfy (at standard pressures and temperatures) the thermodynamic considerations:

$$E_{Zn^{2+}/Zn} = -0.76\,V \qquad E^0_{Cr^{3+}/Cr^{2+}} = -0.41\,V$$

$$E^0_{Mn^{3+}/Mn^{2+}} = 1.51\,V$$

A mixture of electrolytes with the composition 0.1 M $ZnSO_4$ and 0.1 M $MnCl_2$ or 0.1 M $ZnSO_4$ and 0.01 M $CrCl_3$ in the above cell produces significant deviations in the diffusion layer relaxation and in the development of concentration–time profiles, which are presented in this paper, supporting the paramagnetic fluid postulate. A solution of 0.1 M $CrCl_3$ was too highly coloured to allow visible fringes to be formed. Experiments with 0.01 M $MnCl_2$ gave comparable results but are not reported here.

0021-891X/90 $03.00 + .12

A further discovery is that increased mass transport, obtained by appling a magnetic field to a zinc electrolyte containing added paramagnetic ions, smooths the deposit and avoids dendritic growth, in agreement with other studies [3–5]. This factor has caused serious failures of zinc electrode storage cells [6]. The present magnetic field effect work provides the mass transport data for the above cells. A review of the current status of magnetoelectrolysis reveals the need for concerted investigation into the phenomenon [7], since it seem likely that large, inexpensive superconducting magnets with large fields across large cavities will probably be available in the foreseeable future.

2. Experimental details

All experiments were conducted using a 225 Keithley current source for delivering a constant current to the cell. The progress of the electrolysis was monitored by a periodic measurement of the impressed voltage (127 A Keithley). Current densities were adjusted in steps from 0.10 to 7 mA cm^{-2}. The interferograms were recorded with a 35 mm Nikon camera. The entire experiment was videotaped through the Nikon camera optics using a RCA video camera (CC030), Hitachi video recorder (VT-7A) and a Hitachi 20-inch (51 cm) colour video monitor. Several experiments were also performed using a Hitachi video camera (Saticon VK-C870), A Hitachi video recorder (VT-6500A) and a 20-inch Electrohome video monitor. In general, the video display on the various monitors was at a magnification of 20–50 ×.

The cell holder employed was described in [1, 2, 8–13]. It was made of brass with two square flanges with three screws to hold the electrolytic cell and adjust the wedge angle. The cell was placed in the magnet pole gap (about 5 cm) with a convenient arrangement to tilt the cell for obtaining good fringes. The light source (1 mW He–Ne laser) was mounted on a precision lathe bed which had horizontal and vertical vernier movements. The light source was kept 1.3 m from the magnet to avoid field effects on the plasma. The absence of field effects on the refractive index of the solution was confirmed by noting the fringe pattern changes (none) with and without magnetic field. All experiments were carried out at room temperatures (22 ± 0.5° C).

The experiments were performed in different electrode orientations with respect to the magnetic field and the Earth's gravitational field. In the V-position the magnetic field was parallel to the electric field and in the A/C- or C/A-position the magnetic field was perpendicular to the electric field. The distance between the two zinc electrodes was fixed at 2.5 or 4.00 mm. The interferometric cell used in the present studies was described in [8–11]. The shape of the Zn electrodes was semicircular to fit into the short, cylindrical Teflon cell and they were 3 mm thick. The sides of the electrodes, except the parallel faces, were insulated by a sprayed-on coating of glyptol. The electrochemical cell itself acted as a Fabry–Perot interferometer which contained the zinc electrodes and the elecrolyte.

Zinc sulphate ($ZnSO_4 \cdot 7H_2O$) was obtained from Sigma Chemicals. Other chemicals were from the McArthur Chemical Co. ($MnCl_2 \cdot 4H_2O$), BDH Laboratories ($CrCl_3 \cdot 6H_2O$) and Na_2SO_4 Analar grade.

Galvanostatic electrolysis was performed at selected current densities and the relative position of the fringes was recorded at 30, 60, 120, 180, 240, 300, 360 and 600 s. The experiment was repeated by applying an external magnetic field and the fringes were recorded at the above intervals. The relaxation times were always measured by filling the cell with a fresh electrolyte solution before applying the magnetic field and electrolysing.

The recorded frames were analysed on a plotting table and hand-drawn on large sheets of millimetre graph paper at 18 × magnification. The fringe shifts were converted to concentration contours from the well-known correlations between refractive index and concentration with an accuracy of approximately ± 1%.

The analysis of the interferometric fringes was also carried out using a camera reader (camera head, C-1000 Hamamatsu), camera control (Hamamatsu C-1000) and a PDP-11-03-01 computer. The fringes generated and the data from them were essentially identical to the data produced manually.

Lycopodium particles were added to all cells where convection was expected and selected particles followed through more than ten video frames to calculate a vertical or horizontal velocity. No attempt was made to measure or calculate the velocities into or out of the cell.

3. Results and discussion

3.1 *Zn/ZnSO₄/Zn*

3.1.1. V-position. The growth of concentration gradients during the electrolysis at 0.59 mA cm^{-2} in the presence and absence of the magnetic field is shown in Fig. 1. The fluid velocity at the anode, where the concentration of ions is higher, would be expected to be greater than at the cathode. Colliphonium particle tracking did not show this, presumably because the particles followed were not in the highest velocity stream, which is very close to the electrode. However, the fringe shift near this electrode was less than at the cathode, an indication of greater local velocity. Some of the loss of fringe shift is, however, due to optical effects; that is, in an increasing concentration (and refractive index) gradient the light is deflected towards the electrode and, therefore, the fringe end is foreshortened by being cut off by the opaque electrode [14]. The concentration–time plot for the cathode for this electrolysis (maximum concentration change) is shown in Fig. 2. From the interferograms (Fig. 3), it is evident that the concentration gradients are higher (at the anode) in the presence or absence of the applied

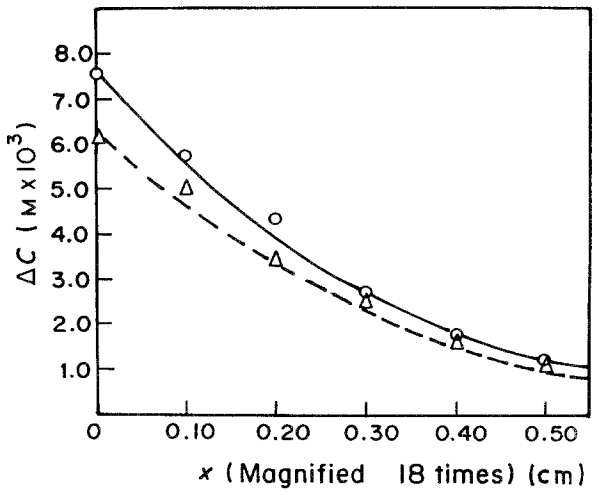

Fig. 1. Plot of changes in concentration (ΔC) against distance in cm (from the electrode surface) at $i_0 = 0.59\,\text{mA cm}^{-2}$ in the presence and absence of a magnetic field in the V-position for the electrolysis of Zn^{2+}. The elapsed time of electrolysis is 240 s (cathode); (△) $H = 0.435\ T$ (○) $H = 0$, $Zn/ZnSO_4/Zn$.

magnetic field. In Fig. 3b at low current density and H = 0 the concentration profile is steeper, but the fringe shift is approximately the same. Approximate symmetry is lost at the higher ($7.6\,\text{mA cm}^{-2}$) current density. This and the concentration profile at the cathode (Fig. 3a) is slightly increased in extent and magnitude in the field, perhaps due to field effects on the diamagnetic Zn^{2+}. These results should be compared with the fluid flow observed in the magnetic field for $Cu/CuSO_4/Cu$ [1] where a more rapid flow was detected by suspended particles and less-extensive diffusion layers were shown by the fringe system.

Upon termination of the electrolysis the diffusion layer slowly relaxes and, as a result, the fringes return to their normal unbent positions seen before the start of electrolysis. The relaxation times ranged from 1 to 2 min and were faster when the magnetic field was applied to the cell. For $i_0 = 1.11\,\text{mA cm}^{-2}$, $\tau = 2\,\text{min}$ 08 s ($H = 0.435$ T). Velocities obtained for other solutions by following lycopodium particles through

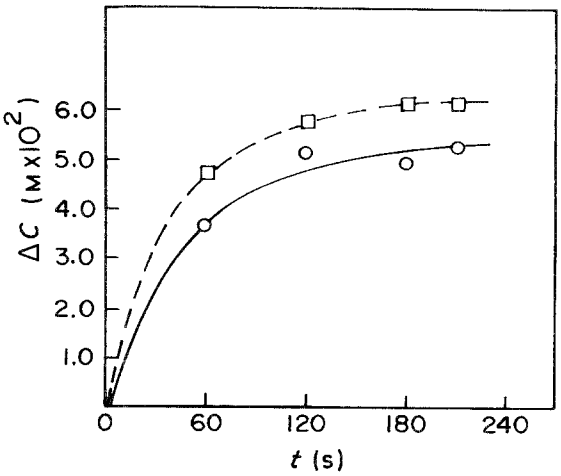

Fig. 2. The concentration changes (ΔC) at the electrode surface plotted against time in the presence o^ a magnetic field of (○) $H = 0.435\ T$ and (□) $H = 0$ at $i_0 = 0.5\upsilon\,\text{mA cm}^{-2}$ in the electrolysis of Zn^{2+} in the V-position (cathode).

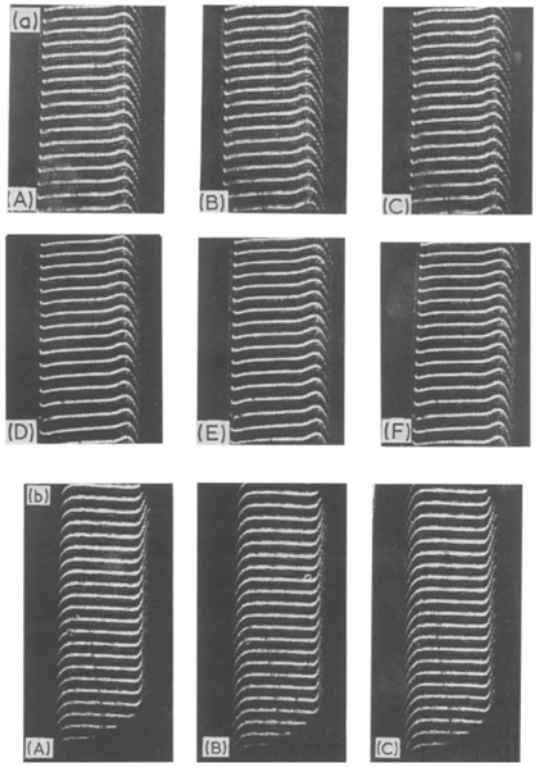

Fig. 3. (a) Laser interferogram recorded in the electrolysis of $ZnSO_4$ at zinc electrodes at $i_0 = 7.6\,\text{mA cm}^{-2}$ in the presence and absence of a magnetic field in the V-configuration. A 60 s, B 120 s, C 180 s, $H = 0$, and D 60 s, E 120 s, F 180 s, $H = 0.435$ T. The anode is on the left. The electrode separation 2.5 mm. (b) Laser interferograms recorded in the electrolysis of $ZnSO_4$ at zinc electrodes at $i_0 = 0.59\,\text{mA cm}^{-2}$ at $H = 0$. A 60 s, B 120 s, C 600 s. The anode is on the left. The electrode separation is 2.5 mm.

at least ten frames was not possible in this solution. Several trials were made and several particles followed for several frames and an estimated velocity constructed from these incomplete data.

3.1.2. C/A-position. The galvanostatic electrolysis in this configuration generated a smooth bending of the fringes at both the electrodes, which progressively increased with time. Unlike in the V-position, where a small fringe shift difference ($\Delta\Delta F_x = 0.5$) was observed due to the natural convection in the two electrode regions, the fringe shifts were identical in this configuration. In a typical run with a current density of $1.11\,\text{mA cm}^{-2}$, a fringe shift after 360 s was 1.3, corresponding to a $\Delta C = 1.05 \times 10^{-2}$ M at the anode and an identical value was obtained for the cathodic fringe shift. When electrolysis was performed at higher current densities such as $7.71\,\text{mA cm}^{-2}$, a small difference in the fringe shifts at the electrodes was observed (at cathode $\Delta F_{\text{Max}} = 1.86$ corresponding to 1.50×10^{-2} M and anode $\Delta F_{\text{Max}} = 2.00$ corresponding to 1.62×10^{-2} M), probably resulting from optical effects [14]. The magnetic field did not promote a significant difference in the electrolysis in this configuration.

Experiments were conducted at current densities of 0.22, 0.55, 1.11 and $2.22\,\text{mA cm}^{-2}$ for a period of 360 s and the relaxation of the fringes was followed after termination of the electrolysis both in the absence and

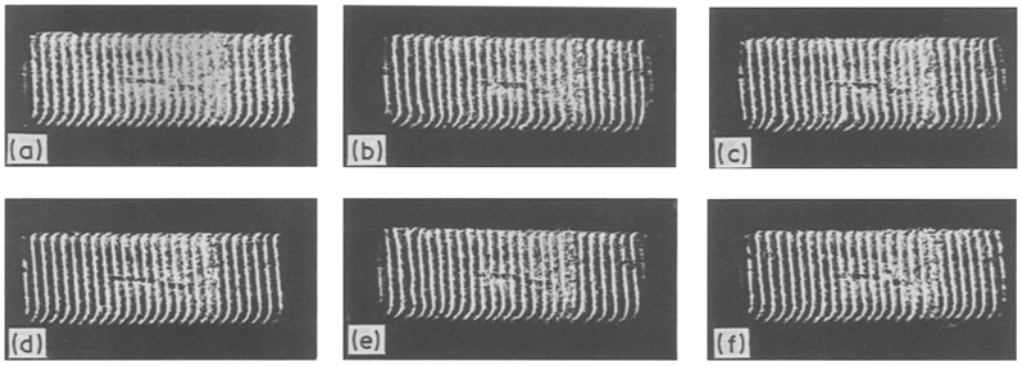

Fig. 4. Development of convection during the electrolysis of $ZnSO_4$ at $i_0 = 0.59\,mA\,cm^{-2}$ in the A/C configuration in the presence and absence of a magnetic field. For panels a–c, $H = 0$, d–f $H = 0.43\,T$ at 60, 120 and 360 s. The electrode separation is 2.5 mm.

in the presence of magnetic field. At all current densities the relaxation times, τ, were unaffected by the field, at $0.22\,mA\,cm^{-2}$, $\tau = 3\,min\ 48\,s$ ($H = 0$) and $t = 3\,min\ 46\,s$ ($H = 0.15\,T$) and $0.55\,mA\,cm^{-2}$, $\tau = 5\,min\ 49\,s$ ($H = 0$) and $\tau = 5\,min\ 39\,s$ ($H = 0.15\,T$), at $1.11\,mA\,cm^{-2}$, $\tau = 8\,min\ 50\,s$ ($H = 0$) and $\tau = 8\,min\ 53\,s$ ($H = 0.15\,T$). This behaviour did not change at higher magnetic field strengths. Some values are plotted in Fig. 5, below.

3.1.3. A/C-position. The concentration profiles in this configuration are highly distorted (left side of fig. 4, panel c) due to the fluid flow from the anode to the cathode. These interferograms were recorded during the electrolysis at a current density of $0.59\,mA\,cm^{-2}$. The effect of the magnetic field on the relaxation was significant. Generally, the relaxation of the fringes is slower in this configuration with the application of magnetic field during electrolysis and relaxation. Figure 5 shows a plot of τ against applied magnetic field; at a current density of $0.22\,mA\,cm^{-2}$, $\tau = 46\,s$ ($H = 0$) and $\tau = 1\,min\ 2\,s$ ($H = 0.52\,T$); at $0.55\,mA\,cm^{-2}$, $\tau = 1\,min\ 19\,s$ ($H = 0$) and $\tau = 3\,min\ 4\,s$ ($H = 0.52\,T$).

3.2. $Zn/ZnSO_4 + MnCl_2/Zn$

3.2.1. V-position. The growth of interference fringe shifts during electrolysis at current densities ranging from 0.10 to $7.0\,mA\,cm^{-2}$ showed significant magnetic field effects. The fringe distortions were noticeable at all current densities examined. Figure 6 shows the plot of impressed voltage against time in the presence and absence of the magnetic field. The impressed voltages were about 40% smaller in the presence of the field. The development of the concentration–time profile during the electrolysis is shown in Fig. 7. In the presence of the magnetic field the concentration gradients are lower than the zero-field value.

The fluid flow velocity in the presence of an applied magnetic field was measured and the values are listed in Table 1. The fluid flows from the anode downwards, and at the cell bottom it moves horizontally towards the cathode. The fluid flow direction is shown schematically in Fig. 8. One noticeable feature of the fluid flow is the development of several concentric flow cells within the electrolytic cell. These flow pockets have the same uniform velocity. The downward flow and the upward flow velocities are nearly identical; the

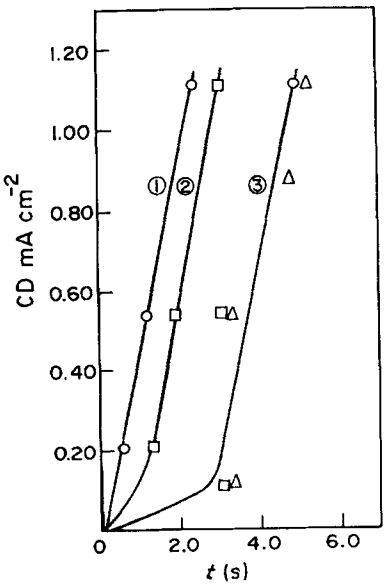

Fig. 5. Plot of relaxation time τ against applied magnetic field in the electrolysis of $ZnSO_4$ (○) $H = 0$, (△) $H = 0$ and (□) $H = 0.52\,T$ in both positions during relaxation and electrolysis, 1 A/C position, 2 A/C position, 3 C/A position.

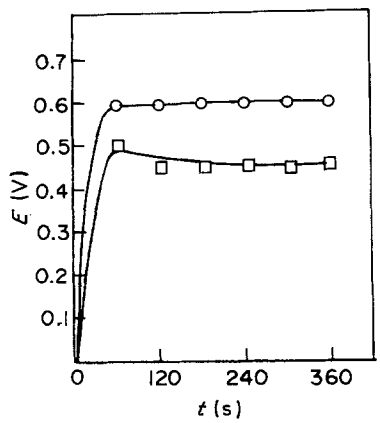

Fig. 6. The impressed voltage against time plot in the presence and absence of a magnetic field for the electrolysis of 0.1 M $ZnSO_4$ in the presence of 0.1 M $MnCl_2$. (○) $H = 0$ and (□) $H = 0.436\,T$, $i_0 = 1.2\,mA\,cm^{-2}$ in the V-position.

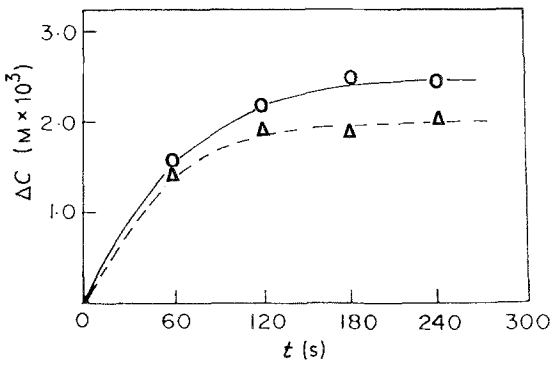

Fig. 7. Concentration–time profile in the electrolysis of 0.1 M $ZnSO_4$ in the presence of 0.1 M $MnCl_2$ at the anode, $i_0 = 0.59\,mA\,cm^{-2}$, (○) $H = 0$ and (□) $H = 0.435\,T$ at $x = 0$.

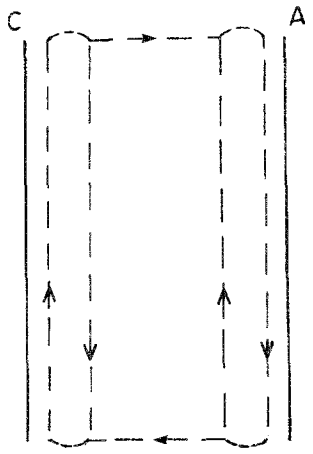

Fig. 8. Fluid flow diagram sketched on the basis of the observed particle movement in the electrolysis of 0.1 M $ZnSO_4$ containing 0.1 M $MnCl_2$. $i_0 = 5.9\,mA\,cm^{-2}$ (V-position).

horizontal flow velocities are lower but not measureable. No attempt was made to measure the rotational (into the plane of the interferograms) velocity which must be considerable. Consistently, the diffusion layer relaxation time was longer in the presence of the magnetic field with paramagnetic ions present. For $i_0 = 0.11\,mA\,cm^{-2}$, $\tau = 1\,min$ ($H = 0$) and $\tau = 1\,min\ 25\,s$ ($H = 4.35\,T$) and for $i_0 = 0.59\,mA\,cm^{-2}$, $\tau = 2\,min\ 4\,s$ ($H = 0$) and $\tau = 3\,min\ 4\,s$ ($H = 0.435\,T$) were observed. The fringes relaxed very smoothly both in the presence and in the absence of the magnetic field. We believe that this is due to the suppression of microturbulance which would retard mixing.

3.2.2. *C/A-position*

Figure 9 shows the interference fringes which were generated during the electrolysis of a mixture of $ZnSO_4$ and $MnCl_2$. The fringe bending in the cathodic and anodic regions was very smooth with a constant growth of the corresponding diffusion layers. However, the growth of the diffusion layers was influenced considerably by the magnetic field (Fig. 10), shown by the marked asymmetry from left to right. The growth of the diffusion layer proceeded in an unlimited fashion as in the case of electrolysis of $CuSO_4$, and the left to right asymmetry again increased. The anode diffusion layer growth progresses leftward (into the field as expected for paramagnetic ions), an effect which was absent during the electrolysis of pure $ZnSO_4$. The diffusion layer grew more rapidly at the cathode in this configuration (C/A). It appears from the results that the paramagnetic ion movement by the applied field may be responsible for the diminished anodic layer, since the indifferent ion concentration increases at the cathode. This effect is greater at longer electrolysis times. The straight centre portion of the fringe system increases its slant to the right (Figs 9d–f) during electrolysis, especially the left side of the frame. This effect is attributed to the paramagnetic ion moving into the magnetic field (to the left). The perturbations beginning at the right side of Fig. 9f are an indication of the onset of convection in this otherwise conventionless arrangement. This panel at 600 s of electrolysis is very different from panel c at $H = 0$ and from the results when Na_2SO_4 was the indifferent electrolyte, as is discussed below. As a result of the rotation of the solution containing paramagnetic ion, the relaxation of the diffusion layers is altered significantly (see later). This is convincing proof that the diffusion layer at the cathode contains Mn^{2+}. There is also a clear indication in the increased fringe bends at the left side of the cell, of migration of the paramagnetic species into the field.

Table 1. Flow velocity in the magnetic field (measured at a current density of about 7.6 mA cm^{-3})

Magnetic field (T)	$V\downarrow$ ($cm\,s^{-1}$)	$V\uparrow$ ($cm\,s^{-1}$)	$V\rightarrow$ ($cm\,s^{-1}$)
Zn/0.1 M $ZnSO_4$/Zn			
0.436	1.2*	1.2*	–
Zn/0.1 M $ZnSO_4$ + 0.1 M $MnCl_2$/Zn			
0.095	1.7	1.4	0.10
0.270	2.3	1.7	–
0.436	7.0	7.0	–
Zn/0.1 M $ZnSO_4$ + 0.01 M $CrCl_3$/Zn			
0.095	1.0	1.3	–
0.270	2.0		–
0.436	4.6	4.6	–

* Estimated; –, not measured.
$V\downarrow$, Downward flow velocity; $V\uparrow$, upward flow velocity; $V\rightarrow$, horizontal flow velocity.

The mass transport coefficient values obtained by analysing the interferograms at different current densities and at different magnetic field strengths are given in Table 2. The results suggests that the mass transport coefficient increases at the cathode and that this increase is higher at higher magnetic field strengths. This also correlates well with the results [10] found with indifferent electrolyte present in these small cells. Since at zero field, mass transport of the ion is diffusion controlled, m_0 values do not appear in Table 2. Figure 11 shows the plot of the impressed cell voltage necessary to produce a given current density, with and without the magnetic field. A slightly decreased impressed potential is required with the field applied to give the equivalent current density.

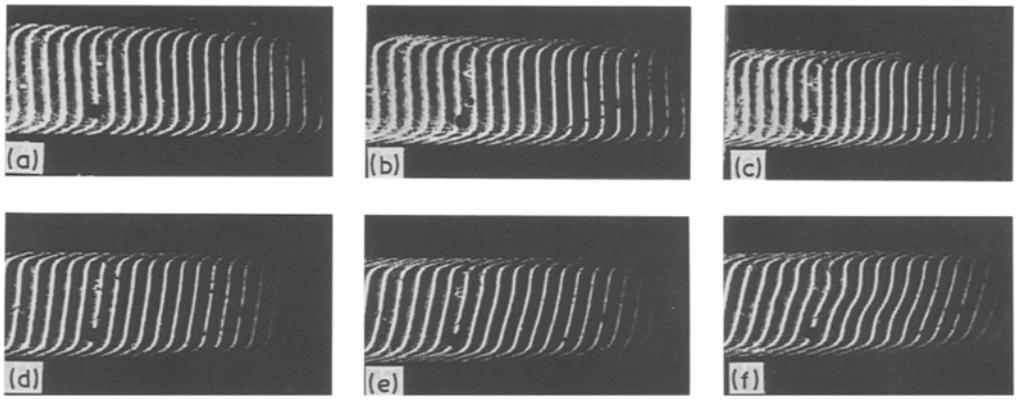

Fig. 9. Laser interferograms produced during the electrolysis of 0.1 M $ZnSO_4$ containing 0.1 M $MnCl_2$. $i_0 = 0.59\,mA\,cm^{-2}$. C/A-position. (top) $H = 0$ and (bottom) $H = 0.435\,T$ a 60 s, b 240 s, c 600 s, d 60 s, e 240 s and f 600 s. The electrode separation is 2.5 mm.

The relaxation time of the diffusion layer in the C/A-position in the presence of the field is increased significantly with paramagnetic ions. The relaxation times in the electrolysis at $0.59\,mA\,cm^{-2}$ for 360 s are: $\tau = 2\,min\ 52\,s$ ($H = 0$), $\tau = 3\,min\ 45\,s$ ($H = 0.094\,T$), $\tau = 4\,min\ 10\,s$ ($H = 0.194\,T$) and $\tau = 12\,min$ ($H = 0.273\,T$). Although the actual values have about a 10% fluctuation between different experimental runs, the above trend remains. A plot of the relaxation time against the applied magnetic field is shown in Fig. 12. The longer relaxation times suggest that relaxation is a more complicated process for paramagnetic ions in a magnetic field.

The only possible explanation in terms of flow mechanics, since no energy (for increased convection flow results) can be obtained from a magnetic field, is that the microturbulence leading to microviscous effects is suppressed and, hence, the apparent viscosity is reduced, allowing increased convection to remove major amounts of concentration polarization. The apparent change in the viscosity caused by the magnetic field can be understood through

$$H_a = BL(\kappa/\eta)^{1/2} \qquad (1)$$

where H_a is the Hartmann number, B is the magnetic susceptibility times the applied field, κ is the electrical conductivity, L is the distance between the electrodes and η is the viscosity. This expression suggests that H_a is decreased in the above experiments in relaxation. The relative increase in apparent viscosity of aqueous solutions in the imposed magnetic field has been observed with KCl solutions [15, 16] — these are diamagnetic. Fahidy and co-workers [7, 17] have discussed the possibility of electrical conductivity changing in the magnetic field and with the solutions employed here, at the current densities operating, this change was considered small (for diamagnetic solutions and not for diamagnetic solutions with strong indifferent paramagnetic ions added; see the voltage–time curves). We have [1, 2] also discussed a decrease in apparent viscosity in a magnetic field under certain circumstances where suppression of microturbulence might be expected to limit energy dispersal and, on relaxation, to prevent the intimate microconvective mixing effective in concentration equalization.

3.2.3. A/C-position. The generally unstable development of convective cells (Fig. 13) was reduced slightly with $MnCl_2$ present and at a field strength of 0.435 T. No meaningful measurement of the concentration gradients were possible and relaxation was not affected by the field; for example, $i_0 = 0.59\,mA\,cm^{-2}$,

Table 2. Apparent mass transfer coefficients of zinc ion in a magnetic field in the C/A-position, 0.1 M $ZnSO_4$ plus other ions*

Field strength (T)	$d^\dagger$ (cm)	i ($mA\,cm^{-2}$)	D ($cm^2\,s^{-1} \times 10^5$)	*Grad* m ($cm^2 \times 10^3$)	m_0 ($cm\,s^{-1} \times 10$)
0.1 M $MnCl_2$					
0.0	0.25	0.26	6.87	2.7	
0.435	0.25	0.26	6.87	3.2	2.20
0	0.25	0.59	6.87	3.2	
0.435	0.25	0.59	6.87	3.5	2.41
0	0.25	1.18	6.87	3.9	
0.435	0.25	1.18	6.87	7.5	5.17
0.01 M $CrCl_3$					
0.0	0.25	0.59	6.87		
0.094	0.25	0.59	6.87	4.7	3.2
0.194	0.25	0.59	6.87	6.3	4.3
0.274	0.25	0.59	6.87	7.3	5.0

*Calculation of m_0 was based on experimentally determined gradients using the formula for mass transfer $J = nF/(1 - t^+)(-D\,\text{grad}\,C + m_0C_0)$, where n is the number of electrons, F the Faraday constant t^+ the transport number and D the diffusion coefficient.

† Electrode separation.

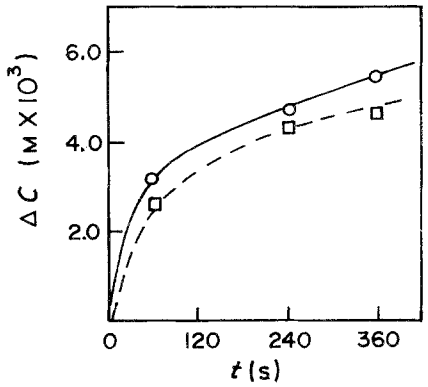

Fig. 10. Concentration changes (ΔC) at the electrode surface during the electrolysis of 0.1 M $ZnSO_4$ containing 0.1 M $MnCl_2$ in an applied magnetic field strength of (□) H = 0.435 T, C/A-position, (○) H = 0, i = 0.59 mA cm^{-2}.

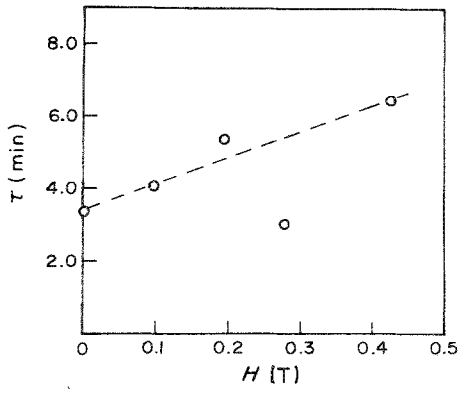

Fig. 12. Relaxation time τ plotted against imposed magnetic field strength in the C/A configuration. The electrolysis time elapsed is 360 s. i_0 = 0.24 mA cm^{-2}.

τ = 1 min 46 s (H = 0), τ = 1 min (H = 0.435 T), τ = 1 min 5 s (H = 0.194 T), i_0 = 1.11 mA cm^{-2}, τ = 1 min 6 s (H = 0) and τ = 1 min 10 s (H = 0.435 T).

3.3. *Zn/ZnSO$_4$ + CrCl$_3$/Zn*

3.3.1 V-position. The general features of this system are similar to the solution containing $MnCl_2$ instead of $CrCl_3$. The highly coloured $CrCl_3$ had to be diluted to 0.01 M to get visible fringes. The fringe shift increased progressively with time at both the electrodes. However, the cathodic fringe shift was always found to be greater than the anodic fringe shift in these specific experiments. Figure 14a shows the laser interferogram of the concentration–time plot for i_0 = 0.59 mA cm^{-2}. In the presence of the field the concentration gradient is slower at any instant (Fig. 14b)

The flow velocities in the V-position have been measured using a suspension of lycopodium particles in the medium at different imposed magnetic field strengths. The data are shown in Table 1. The velocities are smaller than with $MnCl_2$ in the medium. Two possible explanations may be offered: the concentration effect (the concentration of Cr^{3+} ion in the medium is one-tenth of the Mn^{2+} concentration) and because it has only three unpaired electrons to the five of Mn^{2+} and hence is less paramagnetic as a first approximation. The effect would be expected to be proportional in some way to these two variables, but this is not evident.

The impressed voltage–time curves in this configuration in the presence and absence of a magnetic field are shown in Fig. 15. The observed effect is significant due to the effect of the magnetic field increasing the natural convective velocity. Between curves 2 and 3 with only 0.435 T applied, the voltage reduction was about 13%. This should be considered in the light of the rough proportionality [2] found between strength of field and current density in reducing applied potential for a given current density.

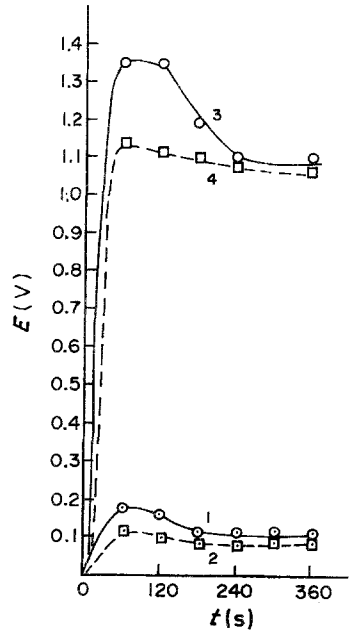

Fig. 11. The impressed voltage plotted against time during the electrolysis of 0.1 M $ZnSO_4$ containing 0.1 M $MnCl_2$ in the C/A configuration. 1 ○ H = 0, 2 □ H = 0.5 T, i_0 = 0.24 mA cm^{-2}, 3 ⊙ H = 0, 4 ⊡ H = 0.5 T, i_0 = 0.06 mA cm^{-2}.

3.3.2. C/A-position. Figure 16 shows the interferograms recorded at a current density of 0.59 mA cm^{-2} at different durations of electrolysis in the presence and absence of magnetic field and 0.01 M $CrCl_3$. As with other systems, here also a smooth growth of fringe shifts was observed during the electrolysis at both the electrodes. The central part of the fringe system is not perturbed by the application of the field but there is, as in Fig. 9, a change in the left side of the figure, probably due to the gathering of the paramagnetic ion into the field. Figure 17 shows the fringe shift analysis for this system. The shape of the concentration–time profiles in the presence of an imposed magnetic field is unchanged; the gradients ($\Delta c/\Delta x$) are sharper in the latter situation, and a sharper gradient develops at higher field strengths. This pattern is very similar to the $Zn/ZnSO_4$ + $MnCl_2/Zn$ system; the smaller effect observed here may be due to the lower concentration of $CrCl_3$ employed (0.01 compared with 0.10 M) above. Because 0.01 M $CrCl_3$ was strongly coloured, thus decreasing fringe visibility, 0.01 M solution was always used.

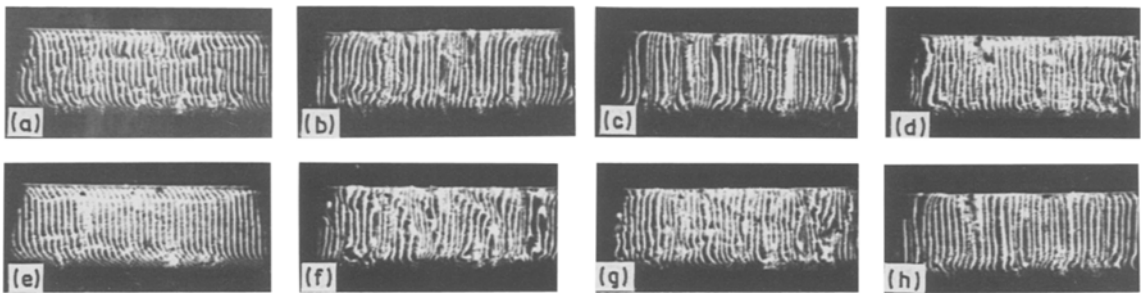

Fig. 13. Onset of convection in the electrolysis of 0.1 M $ZnSO_4$ containing 0.1 M $MnCl_2$ at i_0 = 5.90 mA cm^{-2} in the A/C configuration. H = 0, a 20 s, b 30 s, c 180 s, d 360 s; and for H = 0.435 T, e 20 s, f 30 s, g 180 s and h 360 s. The electrode separation is 2.5 mm.

The mass transport coefficients were evaluated following the procedure described above. The m_0 values shows an increase with increasing magnetic field strengths (see Table 2) and are generally smaller than when $MnCl_2$ was present. This may be due to concentration or the degree of paramagnetism. Figure 18 shows the impressed voltage–time plot in the electrolysis carried out at 0.435 T at i_0 = 0.59 mA cm^{-2}. The voltages in the applied field are slightly higher as they were for the same experiment with paramagnetic Cu^{2+} (compare this curve with that in Fig. 15).

The characteristic diffusion layer relaxation was also monitored after 360 s of electrolysis. Figure 19 shows the plot of τ against the applied magnetic field. The higher relaxation time in the external field is indicative of the paramagnetic fluid flow. The straight centre section (Fig. 16) of the zero field (top interferogram) is parallel for all fringes in the field of view but for H = 0.435 T they exhibit a slight progressive slant into the field at the anode side, showing the slow rotational motion previously noted [1] in paramagnetic electrolytes in the C/A configuration.

3.3.3. A/C-position. Figure 20 shows the development of the concentration profiles which are typically distorted due to the onset of convection. The effect of magnetic field in this configuration has been to reduce this distortion slightly.

On the basis of the data obtained on the three cells described here, the flow of the fluid in the C/A-position is well demonstrated under an imposed magnetic field for the cells $Zn/ZnSO_4$ + $MnCl_2/Zn$ and $Zn/ZnSO_4$ + $CrCl_3/Zn$. There was no perceptible magnetic effect for the cell $Zn/ZnSO_4/Zn$. In the other cell configurations such as V or A/C, the effect is mixed – both fluid flow due to density gradients giving rise to a magnetohydrodynamic effect and the

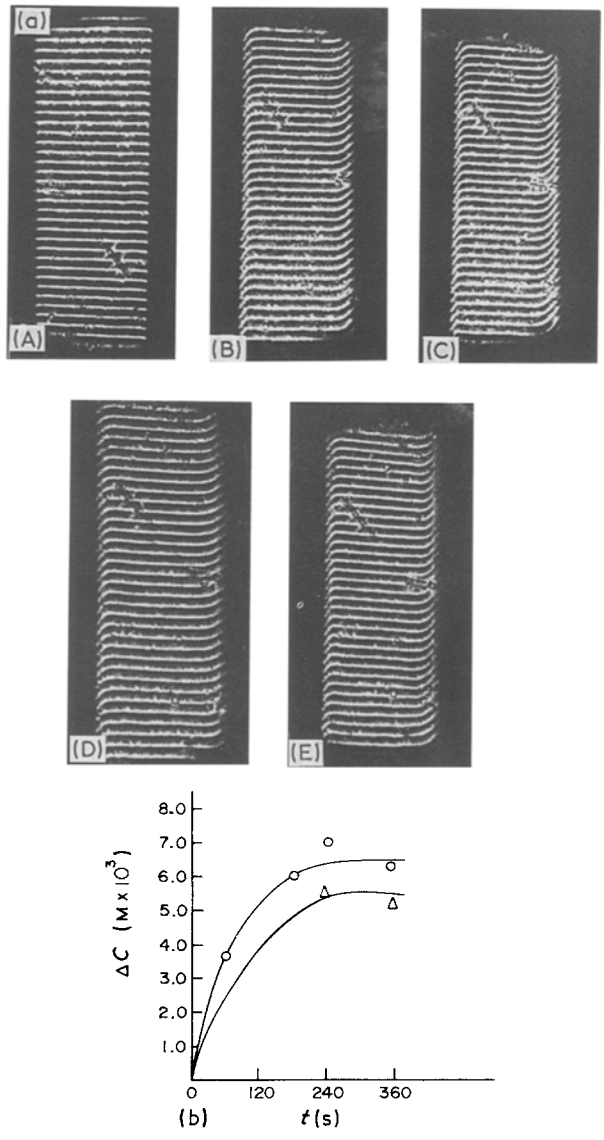

Fig. 14. (a) Laser interferograms recorded during the electrolysis of a solution containing 0.1 M $ZnSO_4$ containing 0.01 M $CrCl_3$ in the presence of magnetic field. A t = 0, H = 0, B t = 60 s, H = 0, C t = 240 s, H = 0, D t = 60 s and H = 0.435 T and E t = 240 s, H = 0.435 T. i_0 = 0.59 mA cm^{-2}, cathode on the left, the electrode separation is 2.5 mm. (b) Concentration changes (ΔC) at the electrode surface during the electrolysis of 0.1 M $ZnSO_4$ containing 0.01 M $CrCl_3$ at i_0 = 0.59 mA cm^{-2} in the V-position. (○) H = 0 and (△) H = 0.435 T.

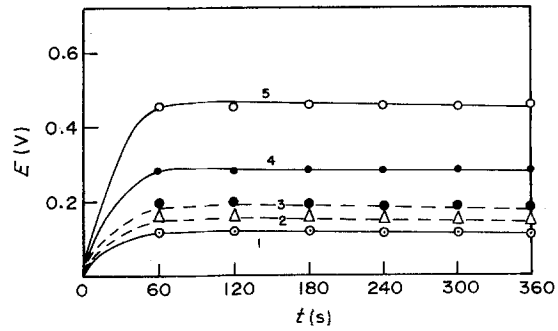

Fig. 15. The impressed voltage against time plot in the electrolysis of 0.1 M $ZnSO_4$ containing 0.01 M $CrCl_3$ in the V configuration, (1) ⊙ 0.2 mA, H = ○, (2) △ 0.5 mA, H = 0.435 T, (3) ●) 0.5 mA, H = 0, (4) • 5.0 mA, H = 0.27 T, (5) 7.5 mA, H = 0.

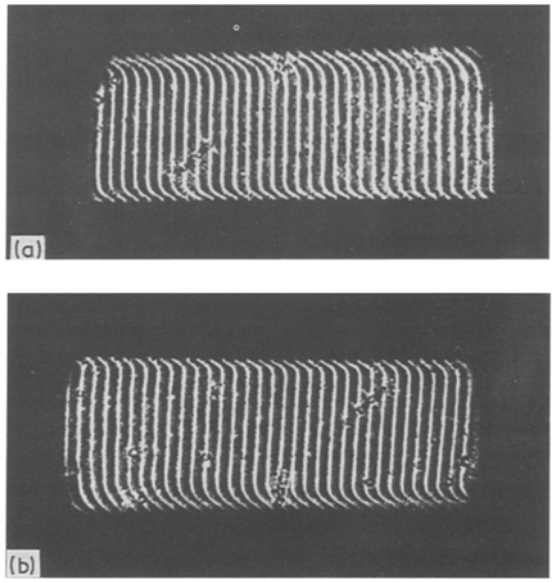

Fig. 16. Laser interferograms in the electrolysis of 0.1 M $ZnSO_4$ containing 0.01 M $CrCl_3$ at $i_0 = 0.59\,mA\,cm^{-2}$. a $H = 0$, b $H = 0.435\,T$. $t = 360\,s$, C/A position.

paramagnetic enhanced fluid flow. The results suggest the formation of a convective diffusion layer at the electrode with the flow direction from electrode to electrode augmented by the paramagnetic ion. The importance of such an increased convective diffusion layer on the restriction of dendrite formation should parallel the effectiveness of impinged fluid flow [5]. The imposed magnetic field might be able to cause an increased fluid flow of equal effectiveness for smooth deposition of Zn.

3.4. $Zn/ZnSO_4 + Na_2SO_4/Zn$

The effect observed in the two electrolytes containing added paramagnetic ions should be absent if a non-paramagnetic ion such as Na^+ is added, so 0.1 M Na_2SO_4 was added. The magnetic field should not affect either the Zn^+ ion or the Na^+ ion to increase convection. The results recorded with and without a field in the C/A-position were essentially identical or no field effect was observed. Examples of results are: at $0.24\,mA\,cm^{-2}$ fringe shifts at the anode and cathode were 1.0 and 1.0, at 180 s and $H = 0$ with concentration gradients of 1.0 and 1.0, with a field of 0.512 T fringe shifts were 1.0 and 1.0 and the concentration gradients 1.0 and 1.1 at the same time and current density. At a current density of 0.59 at 360 s of electrolysis the cathode fringe shifts with and without $mA\,cm^{-2}$ 0.512 T field were identical at 2.75.

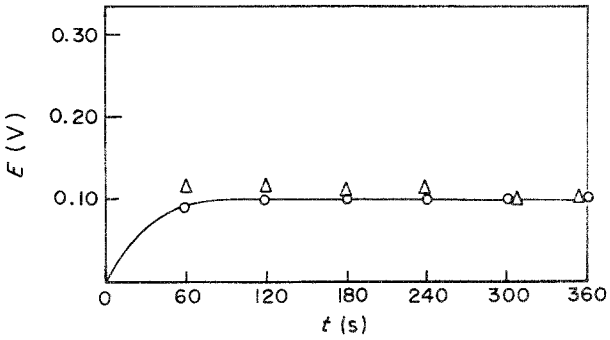

Fig. 18. The impressed voltage against time plot for the electrolysis of 0.1 M $ZnSO_4$ containing 0.01 M $CrCl_3$ during the electrolysis of $i_0 = 0.59\,mA\,cm^{-2}$. (○) $H = 0$ and (△) $H = 0.435\,T$. C/A configuration, at the cathode.

In the V-position, as expected, the magnetic field profoundly affected the interferometric profiles. At a current density of $0.11\,mA\,cm^{-2}$ at 240 and 360 s the fringe shifts were 0.64 and 0.68, respectively, and with 0.512 T applied they rose to 0.80 and 0.88 at the same times at the anode. These results, increased ΔCs, are the reverse of the decreased ΔCs with paramagnetic ion, as is to be expected in a magnetic field.

The influence of an indifferent electrolyte on the transport number of an ion has been well established in the literature. However, although the transport of an ion might be influenced by the inert electrolyte (which has been proven in polarographic diffusion current studies), in the present work we are considering the mass transport effects in a magnetic field during galvanostatic electrolysis. They should be at least in the same direction with inert paramagnetic and diamagnetic ions added if the effect is due to a change in transport number, but in fact are in the opposite direction as required by magnetic theory; that is, paramagnetic ions are attracted into the field and diamagnetic ions repelled.

When an external magnetic field is imposed mass transfer rates are altered significantly [1, 2] by a combination of diffusion and an orderly forced con-

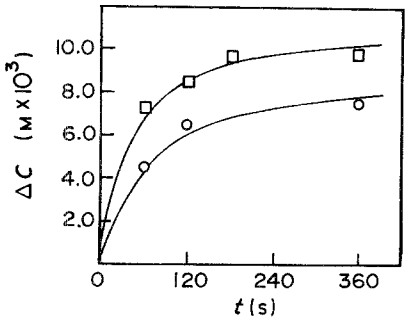

Fig. 17. Plot of concentration changes in the electrolysis of 0.1 M $ZnSO_4$ containing 0.1 M $CrCl_3$ at the electrode surface against time C/A configuration. $i_0 = 0.59\,mA\,cm^{-2}$. (□) $H = 0$ and (○) $H = 0.435\,T$.

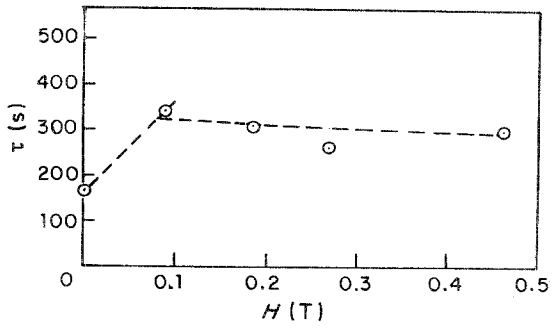

Fig. 19. Relaxation time τ plotted against magnetic field strength for the electrolysis of 0.1 M $ZnSO_4$ containing 0.01 M $CrCl_3$. $i_0 = 0.59\,mA\,cm^{-2}$ and $t = 360\,s$. C/A configuration.

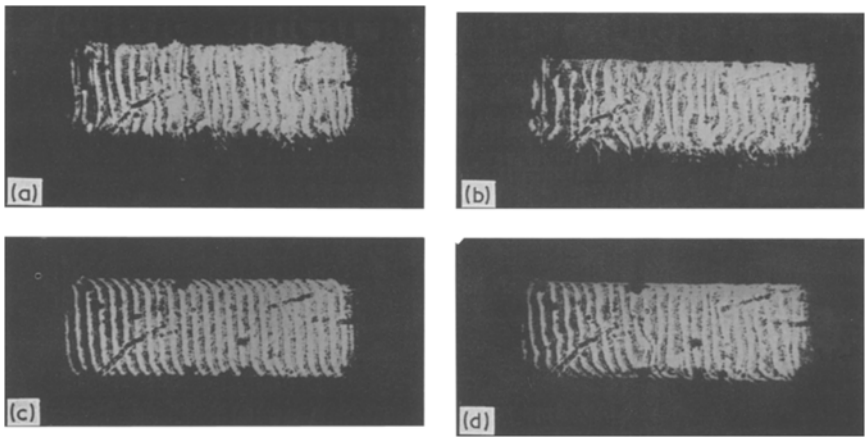

Fig. 20. Development of convection in the electrolysis of 0.1 M $ZnSO_4$ containing 0.01 M $CrCl_3$ in the A/C configuration, i_0 = 5.90 mA cm^{-2}. H = 0 a 60 s, b 360 s, H = 0.435 T, c 60 s and d 360 s.

vection, made visible by the interferograms in the V-position especially. Measurement of the thickness of the diffusion layer, δ (which is now a function of diffusion, natural and forced convection) for mixtures of electrolytes such as $ZnSO_4$ and $MnCl_2$ gives a value of 0.032 cm (at t = 240 s and i_0 = 0.49 mA cm^{-2}) at the cathode in the absence of the field. This is reduced to 0.021 cm when a magnetic field H = 0.435 T is applied to the cell. This trend continues at all other current densities and other magnetic field strengths. In the C/A-position the forced convection is now a low rotation of the magnetic fluid. The diffusion layer thickness is 0.023 cm (H = 0) and t = 360 s at the cathode and 0.043 cm at the anode. When the magnetic field is switched on the thickness is reduced to 0.014 cm at H = 0.435 T at the cathode and 0.028 cm at the anode. The alteration of the diffusion layer thickness occurs very slowly in this position from the very start of the electrolysis and is more prominently observed at the longer electrolysis times. If we take the measured fluid flow velocity (see Table 1) of 7 cm s^{-1} in order to reduce the thickness of the layer by a factor of about 7/10, in the C/A-position the fluid flow velocity would have to be about 5.7 cm s^{-1}. A linear relationship between the fluid flow and the thickness of the diffusion layer has been established in rotating ring disc electrode voltammetry [18–27]. This calculated velocity must be acquired by the fluid because of the paramagnetic ion rotational effect. When the more paramagnetic solution (higher concentration of indifferent paramagnetic cations) in the cathode layer is attracted into the magnetic field starting the rotation (by unequal attraction of the differing concentration of paramagnetic ions at the cathode and anode), a flow of ions down one cell wall and up the other begins so that a right-hand rule magnetohydrodynamic effect reinforces the paramagnetic effect to give the greater velocity observed. It appears that the velocity estimated here cannot be the velocity of the paramagnetic ion effect [18] alone.

Although general support can be obtained in the system containing a mixture of electrolytes such as $ZnSO_4$ and $CrCl_3$ for the above discussion, the extent of this effect is smaller than with $ZnSO_4$ and $MnCl_2$. Diffusion layer thicknesses in the V-position at a current density of i_0 = 0.59 mA cm^{-2} and τ = 240 s, of 0.090 cm (H = 0) and 0.07 cm (H = 0.435 T) were obtained in the cathodic region. It is thus apparent that the growth of the thickness of the diffusion layer depends on the nature of the paramagnetic ion and possibly its refractive index and relative concentration. There is further support in the measured velocities reported in Table 1, where the solution containing $MnCl_2$ was almost twice as effective as the $CrCl_3$ solution.

The diffusion layer relaxation is dependent on the convective flows set up during and after the electrolysis is completed. Since the paramagnetic fluid effect operates in the C/A-position, it is interesting to examine the relaxation behaviour in this configuration. The data shown in Fig. 12 which are in agreement with data previously found for the system $Cu/CuSO_4/Cu$ [1], can be fitted to a linear relaxation equation of the type

$$\tau_H = \tau_0 + kH \qquad (2)$$

where τ_H is the relaxation time in the imposed magnetic field, τ_0 is the relaxation time in the zero field, H is the strength of the applied field and k is a characteristic constant. k has the units of s T^{-1}. Using Equation 2 for the case of $MnCl_2$ and $ZnSO_4$ solution, $k = 4.7 \times 10^{-1}$ s T^{-1}. Equation 2 also appears to be valid for the $ZnSO_4$ + $CrCl_3$ solution, except that there appears to be two types of relaxations; one mechanism operating at low fields with k = 2.0 s t^{-1} and another operating at higher fields with $k = 1.0 \times 10^{-1}$ s T^{-1}. The magnetic field appears to oppose the normal relaxation of the diffusion layer in these sytems or the flows die out. The most probable explanation for the delay in relaxation is that superimposed on the paramagnetic effect driven slow rotation, there is also some convection (in the vertical direction) as shown in Fig. 9, panel f (the kink near the centre of the bulk) and the straight portion of the fringe system from panel d onward is no longer vertical. These two effects, taken together, suggest that the whole of the bulk is now a 'diffusion layer' requiring more time for relaxation than the zero-field experiments where the diffusion layer is clearly defined with the bulk solution unaffected. There is also the case of suppression of microturbulence and hence slowing of the removal of concentration differences.

As previously noted, any energy balance must recognize that no energy can be obtained in a galvanostatic electrolysis from a static magnetic field. We therefore postulate that the field reduces energy dispersion by suppressing microturbulence, giving a lowered apparent viscosity, hence greater convective velocities, reducing concentration polarization. Two effects, magnetohydrodynamic and paramagnetic, contribute constructively. Values given above are for in-plane velocities, other velocities cannot now be measured. Some orientations of the electrodes in the gravity magnetic and electric fields, such as C/A and A/C, are difficult to quantify satisfactorily and measurement of ΔCs are tentative or absent.

4. Summary

(1) In a simple zinc sulphate electrolyte, the magnetohydrodynamic effect at vertical electrodes results in about one-fifth of the vertical velocities found when paramagnetic ions (Cu^{2+}, Mn^{2+} or Cr^{3+}) are present. To the best of our knowledge, this is the first study of the paramagnetic effect in electrolysis [1].

(2) Impressed voltages are reduced when paramagnetic ions are present.

(3) The reduction in applied potential is approximately proportional to the product of the current density and the magnetic field strength.

(4) In the A/C-position the applied potential is reduced by a magnetic field, probably by increasing the convective rate of charge transfer in convection cells of the Bénard type.

(5) In the C/A-postion there is no measurable effect of the field when no paramagnetic ions are present, but with any of Cu^{2+}, Mn^{2+} and Cr^{3+} the solution is a magnetic fluid. The magnetic fluid is attracted into the magnetic field, resulting in a slow clockwise rotation of the electrolyte.

(6) When electrolysis is abruptly discontinued, but the magnetic field remains on the cell, the relaxation of the concentration gradients is retarded compared with zero-field relaxation. It is postulated that this is due to suppression of microturbulence by the field which is effective in destroying concentration differences. Another explanation may be, from the Hartmann equation, that the apparent viscosity is increased or decreased by the magnetic field under some circumstances.

(7) There is a clearly demonstrated paramagnetic effect interacting in a way, as yet unknown in detail, with the magnetohydrodynamic effect; this is substantiated by the findings with the diamagnetic ion Na^{+}.

(8) Further study is necessary to understand fully:
(a) the effects in the A/C-position;
(b) the relaxation effects;
(c) how present mathematical treatments for concentration profiles must be altered to take account of horizontal velocities in magnetic fields;
(d) how presented mathematical treatments must be altered to account for visible effects in the A/C-position in magnetic fields;
(e) A more detailed energy balance should be sought. Since no energy can be obtaind from a static magnetic field (when an elecrochemical reaction is driven by a static parallel electric field), only a reduction in energy dispersal can explain the results. The suppression of microturbulence dispersive processes by the magnetic field seems the most likely explanation. Less microturbulence dispersion of energy would appear as an apparent reduced visosity, resulting in greater convection and lower internal resistance.

Acknowledgements

The authors thank the Natural Sciences and Engineering Research Council for their support and TRIUMF for offering facilities for carrying out this work. We also thank D. E. Lobb for some illuminating conversations, The authors shows their appreciation to Teddy Robert Gathwright for servicing the magnet.

References

[1] R. N. O'Brien and K. S. V. Santhanam, *J. Electrochem. Soc.* **129** (1982) 1266.
[2] *Idem, Electrochim. Acta* **32** (1987) 1679.
[3] J. L. Barton and J. O. M. Bockris, *Proc. R. Soc. A* **268** (1962) 485.
[4] J. T. Kim and J. Jorne, *J. Electrochem. Soc.* **127** (1980) 8.
[5] R. Fratesi, G. Roventi, M. Maja and N. Penazzi, *J. Appl. Electrochem.* **10** (1980) 765.
[6] J. Horne, Y. J. Lii and K. E. Yee, *J. Electrochem. Soc.* **134** 1399.
[7] T. Z. Fahidy, *J. Appl. Electrochem.* **13** (1983) 553.
[8] R. N. O'Brien and K. S. V. Santhanam, *J. Electrochem. Soc.* **129** (1982) 1266.
[9] *Idem, ibid.* **130** (1983) 1114.
[10] K. S. V. Santhanam and R. N. O'Brien *J. Electroanal. Chem.* **160** (1984) 377.
[11] R. N. O'Brien and W. Michalik, *Can. J. Chem.* **61** (1983) 2316.
[12] R. N. O'Brien B. B. Kulkarni W. Michalik and K. S. V. Santhanam, *Can. J. Chem.* **59** (1981) 1933.
[13] R. N. O'Brien and L. M. Mukherjie, *J. Electrochem. Soc.* **111** (1964) 1358.
[14] F. R. McLarnon, R. H. Muller and C. W. Tobias, *ibid.* **122** (1975) 59.
[15] J. Lielmezs and H. Aleman, *Thermochim. Acta* **18** (1977) 315.
[16] J. Lielmezs *Tech. Apskats* **79** (1977) 2.
[17] A. Olivier and T. Z. Fahidy, *J. Appl. Electrochem.* **12** (1982) 417.
[18] Yu. V. Pleskov and V. Yu Filinovskii, 'The Rotating Disc Electrode', Consultants Bureau, New York (1976) Ch. 2.
[19] L. A. Dorfman, 'Hydrodynamic Drag and Heat Transfer at Rotating Bodies', Fizmatgiz, Moscow (1960).
[20] E. C. Cobb and D. A. Saunders, *Proc. R. Soc.* **236** (1956) 343.
[21] B. B. Kulkarni and K. S. V. Santhanam, *Trans. SAEST* **11** (1976) 89.
[22] D. R. Davis, *Quart. J. Mech. Appl. Math.* **12** (1959) 151.
[23] V. G. Levich, 'Physico Chemical Hydrodynamics', Prentice-Hall, Englewood Cliffs, New Jersey (1962).
[24] *Idem, Zh. Fiz. Chim.* **18** (1944) 335.
[25] D. Rosner, *J. Electrochem. Soc.* **113** (1966) 624.
[26] A. C. Riddiford, *ibid.* **108** (1961) 610.
[27] N. Ibl, *ibid.* **108** (1961) 610.